Atmospheric Pollution Research 5 (2014) 753-758

Atmospheric Pollution Research

www.atmospolres.com

Comparison of number, surface area and volume distributions of particles emitted from a multipoint port fuel injection car and a gasoline direct injection car

Gang Lv [1], Chong–lin Song [1], Suo–zhu Pan [2], Jun–hua Gao [1], Xiao–feng Cao [1]

[1] *State Key Laboratory of Engines, Tianjin University, Tianjin, 300072, China*
[2] *School of Transportation and Automotive Engineering, Xihua University, Chengdu, 610039, China*

ABSTRACT

A chassis dynamometer study was conducted to compare the characteristics of particle emissions from a port fuel injection (PFI) and a gasoline direct injection (GDI) car, both of which comply with Euro 4 exhaust emission standards. Experiments were carried out over the New European Driving Cycle (NEDC), the ECE–15 segments, the period from 0 to 49 s within the NEDC procedure (FSE) and the Extra Urban Driving Cycle segment. Exhaust particles were characterized in terms of the particle number, surface area, volume and size distributions between 30 nm and 1 µm. Under the NEDC, the GDI car had particle emissions weighted by particle number, surface area and volume that were 56–2 739% higher than the emissions from the PFI car in the range of particle size measured, and the particle number, volume and surface area emissions per km for the GDI car are respectively 5.3, 9.0 and 14.6 times higher than those for the PFI car. Among the testing conditions employed, the highest concentrations of average particle number, surface area and volume were found in the FSE, and the particle number, surface area and volume for the GDI car were respectively 9.5, 33.2 and 39.8 times higher than those for the PFI car. Moreover, the peak of the particle size distributions for the PFI car was toward a smaller size, while that for the GDI was toward a larger size, indicating that particles emitted by the PFI car are much smaller than those emitted by the GDI car.

Keywords: *Gasoline direct injection car, multipoint port fuel injection car, particle number distribution, particle surface area distribution, particle volume distribution*

Corresponding Author:
Chong–lin Song
☎ : *+86-22-27406840*
🖷 : *+86-22-27403750*
✉ : *songchonglin@tju.edu.cn*

Article History:
Received: 23 January 2014
Revised: 31 May 2014
Accepted: 31 May 2014

doi: 10.5094/APR.2014.084

1. Introduction

There has been increased concern about health issues related to airborne fine particulate matter (PM) in recent years. Epidemiological studies suggest that these fine particles penetrate the human respiratory system rapidly, travel from the lungs to blood tracts and even to the brain, and cause respiratory problems and death (Peters et al., 2000; Samet et al., 2000; Hoek et al., 2002; Li et al., 2003; O'Connor et al., 2008). In many countries, therefore, the emphasis of air quality regulation has progressively moved from airborne total suspended particles (TSP) to PM_{10} (particles with an aerodynamic diameter of less than 10 µm) to $PM_{2.5}$ (particles with an aerodynamic diameter of less than 2.5 µm) (Yin and Harrison, 2008).

Vehicles are one of the most important contributors to airborne fine particles, and a number of pieces of legislations that limit PM emissions from vehicles have been enacted for many years. Traditionally, these regulations only focus on the PM mass emissions from diesel–powered vehicles because the PM emissions from gasoline engines are much lower in mass than those from diesel engines (Eastwood, 2008). However, the European Commission introduced a limit of 6×10^{11} particles/km to GDI cars registered after September 2017, and a laxed limit of 6×10^{12} particles/km at Euro 6 stage in September 2014 (Mamakos et al., 2013a). As a consequence, the number–weighted particle emissions from gasoline engines have recently received particular attention.

Gasoline–fueled vehicles are primarily powered by conventional multipoint port fuel injection (PFI) engines and gasoline direct injection (GDI) engines. Typically, number–weighted total particle emissions are roughly on the order of 10^{12} particles/km for PFI engine vehicles and 10^{13} particles/km for GDI engine vehicles (Eastwood, 2008), and these values are generally lower than those for conventional light–duty diesel vehicles ranging 10^{13}–10^{14} particles/km (Andersson et al., 2001). Moreover, the number–weighted solid particle emissions are typically on the order of 10^{12}–10^{13} particles/km for GDI and 10^{11}–10^{12}particles/km for PFI cars, and those from diesel cars are on the order of 10^{13}–10^{14} particles/km (Mamakos et al., 2013b). Nevertheless, when gasoline engine operating parameters (e.g., the fuel/air equivalence ratio, fuel injection timing, spark timing, engine load and speed and engine operation mode) are varied, the exhaust particle number concentration can increase remarkably. Andersson et al. (2001) and Gupta et al. (2010) reported that exhaust particles from both PFI and GDI engines shoot up dramatically in number concentration and switch from accumulation to nucleation mode as the engine speed or load increases. Kayes and Hochgreb (1999) found that the PM number concentration for a PFI engine increases by as much as three orders of magnitude when the air/fuel ratio either increases or decreases by 30% from stoichiometric ratio. Price et al. (2006) discovered that advancing the spark timing or retarding the injection timing of a GDI engine increases the particle number by more than one order of magnitude. Maricq et al. (1999a) examined the number and size emissions of particles from a production GDI engine over a range of engine operating conditions. They suggested that besides the fuel injection timing, spark timing, engine speed and engine load, the engine operation mode also strongly affects the PM number emission, and found that the particle number emission increases by a factor of about 10–40 as the engine transfers from a homogeneous to stratified operation mode. It is thus important to better understand particle emissions from modern gasoline–powered vehicles.

The current paper mainly focuses on the comparative characteristics of particles emitted from PFI and GDI gasoline cars that have almost the same engine displacement and meet Euro 4 emission regulations (see Table 1). Tests were carried out according to the New European Driving Cycle (NEDC), and the number, surface area and volume distributions of particles emitted from both cars were measured and evaluated using an electrical low–pressure impactor (ELPI).

2. Experimental Section

2.1. Test cars and experimental fuel

Two different types of gasoline cars with almost the same engine displacements were employed in this study. The first one was equipped with a conventional PFI gasoline engine, which was manufactured by Chery Automobile Company Limited. The second one was equipped with a GDI engine, which was manufactured by FAW–Volkswagen Automotive Company Limited. Important specifications and actual gaseous emission data for the cars are given in Tables 1 and 2, respectively. An ultra low–sulfur gasoline fuel was used for the testing. The main properties of this fuel are listed in Table 3.

2.2. Experimental setup and particle measurement

Figure 1 is a schematic diagram of the experimental setup. A climate–controlled test cell (SD530, WEISS) was employed to condition the temperature, pressure and relative humidity in the laboratory. According to the Type 6 test (i.e., cold start test) in the China 4 and Euro 4 emission regulations, the temperature chosen for the NEDC test was conditioned at 266 K. The pressure and relative humidity in the laboratory were conditioned at 1.01×10^5 Pa and 60%, respectively. A chassis dynamometer (RPL220, AVL) operating over the NEDC was used to reproduce real–world on–road driving conditions for the PFI and GDI cars. Exhaust particulates were measured by a real–time particle measurement system, which was composed of a first dilution system, second dilution system, heater, filters, compressor, electrical low–pressure impactor (ELPI, Dekati) and vacuum pump. Exhaust gas in the PFI/GDI car plume was drawn into the first dilution system by a stainless–steel tube (diameter 50 mm), and diluted with the first stage of dilution air, which was heated to 463 K by a heater. The diluted exhaust gas was then diluted again in the second dilution system (temperature of 298 K) and pumped into the ELPI by the vacuum pump. The total dilution rate was set at 64:1. Both dilution airs were supplied by the compressor and filtered by two filters. The conditions of the sampling system should minimize the volatile nucleation mode formation; however, semi–volatile nucleation mode formation at the outlet of the diluters cannot be excluded.

The ELPI is a real–time analyzer with resolution frequency of 1 Hz at a sampling gas flow rate of 10 L/min. It cuts the particles into 12 size fractions over a particle size range from 0.03 to 10 µm (D50% cut size diameters) according to the particle aerodynamic equivalent diameter for a uniform density. The ELPI consisted of a cascade impactor, unipolar diode and multichannel electrometer. During the measurement process, particles were charged with charged ions in the unipolar diode charger and then piped into the cascade impactor with 12 stages. Particles were collected at each stage according to their inertia. The multichannel electrometer was used to measure the current carried by collected particles at each stage. ELPI data were processed manually using ELPIxls data processing software (version 4.01), which calculated the particle number, surface area and volume from the measured values.

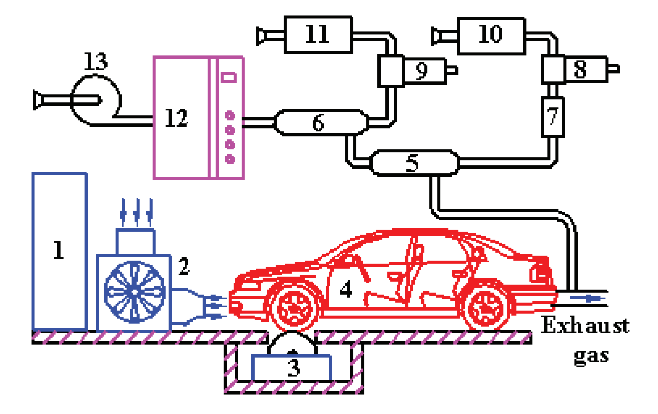

Figure 1. *Setup of particulate matter measurement.* ***(1)*** *Environmental control system,* ***(2)*** *Cooling fan,* ***(3)*** *Chassis dynamometer,* ***(4)*** *PFI/GDI car,* ***(5)*** *First dilution,* ***(6)*** *Second dilution,* ***(7)*** *Heater,* ***(8)*** *,****(9)*** *Filter,* ***(10)*** *,****(11)*** *Compressor,* ***(12)*** *ELPI,* ***(13)*** *Vacuum pump.*

2.3. Experimental protocol

The driving cycle employed in this experiment was the NEDC, which has been applied in emission certification tests of light–duty cars in Europe since 2000. The NEDC consists of four repeated ECE–15 segments (4 × 195 s) without interruption and one Extra Urban Driving Cycle (EUDC) segment (400 s). According to the driving profiles of the NEDC, exhaust particle measurements were made for the first ECE–15 segment (ECES1), the second ECE–15 segment (ECES2), the third ECE–15 segment (ECES3), the fourth ECE–15 segment (ECES4), the first segment of ECES1 (FSE, i.e., the period from 0 to 49 s in the NEDC procedure) and the EUDC. Before running the NEDC experiment, the GDI and PFI cars used were preconditioned with one NEDC and one EUDC. After the preconditioning treatment, the two cars were soaked at a temperature of 266±3 K over 12 hours. Figure 2 is a detailed depiction of the driving profiles used in this study. Experiments were carried out twice under the NEDC, and the average values were used. The relative errors between the average values and the experimental data were all below 8.0%.

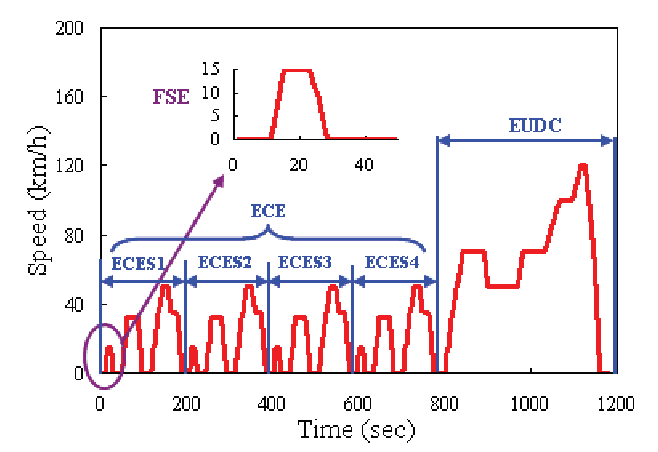

Figure 2. *Driving profiles of the NEDC.*

Table 1. *Specifications of test cars*

Car Type	Car Model	Displacement (L)	Inertia Mass (kg)	Mileage (km)	Emission Limit	After Treatment	Fuel
PFI	SQR7180A217	1.792	1 200	3 746	Euro 4	TWC	Unleaded
GDI	SVW7186BJD	1.798	1 360	3 804	Euro 4	TWC	Unleaded

Table 2. *Exhaust emissions from PFI and GDI cars under the NEDC cycle (unit: g/km)*

Car	THC	CO	NO_X	CO_2
PFI	0.080	0.460	0.054	199.176
GDI	0.045	0.155	0.059	189.166
Euro 4 Limits	0.1	1.0	0.08	

Table 3. *Specifications of gasoline fuel*

Properties	
Octane number (RON)	97
Density at 15 °C temperature (kg/m^3)	742.3
Initial boiling point (°C)	30
Final boiling point (°C)	203
Alkenes (vol. %)	8.9
Aromatics (vol. %)	32.6
Benzene (vol. %)	0.63
Sulfur content (mg/kg)	36

3. Results and Discussion

3.1. Particle number, surface area and volume distributions during the NEDC

During the NEDC, time–resolved measurements of particle size distributions were made without interruption over 1 180 s, and the temporal variations of the particle number for both GDI and PFI cars are shown in Figure 3. The particle number concentrations for the GDI car are significantly higher than those for the PFI car during the NEDC, especially in the ECES1 where the high concentration peaks are observed for the GDI car. Interestingly, a huge particle spike is also found at the deceleration of the EUDC for the PFI car. Ronkko et al. (2014) concluded that these particles formed during deceleration mainly originated from lubricant oil.

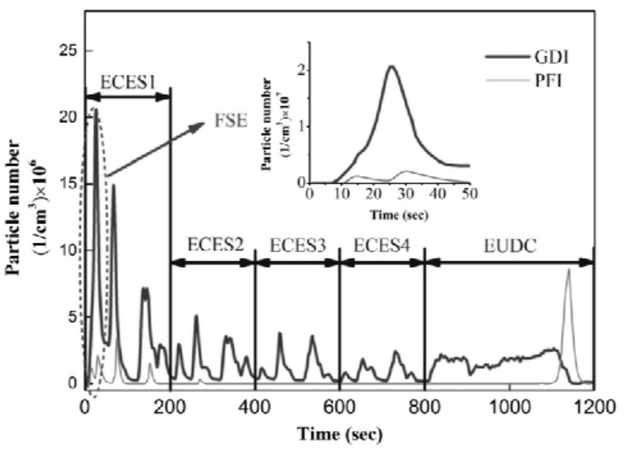

Figure 3. *Temporal variations of the particle number for both GDI and PFI cars under the NEDC.*

The particle number, surface area and volume size distributions measured for the PFI and GDI gasoline cars are shown in Figures 4a–4c, where the plotted particle size is based on the geometric mean of each stage of the ELPI impactor. To evaluate the relative incremental ratios of the particle number, surface area and volume for the GDI car relative to those for the PFI car, the following parameter is used:

$$\varphi_X = \frac{GDI_X - PFI_X}{PFI_X} \quad (1)$$

where, the subscript "*X*" indicates the average particle number (N), surface area (SA) or volume (V).

In Figure 4a, different distributions of the particle number concentrations are observed for the two cars operating under the NEDC. For the PFI car, there is a monotonic drop in the particle number concentration with an increase in particle mean diameter (PMD), while there is a decrease after a slight ascent for the GDI car. The peak particle concentration for the PFI car is below 39 nm, corresponding to the nucleation mode. In the case of the GDI car, the peak value corresponds to the accumulation mode (PMD of ~118 nm). Over the particle size range measured, the φ_N values are 0.57–27.38, implying that the GDI car emits far more particles in number than the PFI car under the NEDC test. Similar results were obtained by Ntziachristos et al. (2004), who found that the particle number concentration for a GDI car is one to two orders of magnitude higher than that for a PFI car. The higher particle number concentration for the GDI car may be ascribed to the adopted combustion mode of the car engine. The multipoint PFI mode of the PFI engine provides a longer time to prepare the air–fuel mixture and eliminates wall wetting (Zhao et al., 1999); this facilitates more complete combustion and fewer particles are produces. By contrast, the inhomogeneous charge combustion mode of the GDI engine reduces the charge mixture time, results in more local rich regions, and increases the number of exhaust particles (Price et al., 2006). Moreover, Liang et al. (2013) measured the particle number distributions from a GDI car and a PFI car, which met the Euro 4 emission regulation, over the NEDC using an ELPI. For the PFI car, the trend of particle number distributions obtained in this study is similar to their results. However, the particle number distributions for the GDI reported by Liang et al. (2013) showed a monotonic decrease with the increase of particle size, which is in conflict with our results. The reasons for this phenomenon are probably attributable to the differences in controlling strategy of engines, combustion chamber's geometry, intake swirl ratio, chemical compositions of the fuel and catalyst etc., which can cause the different experimental results.

Figure 4b presents the particle surface area per unit volume of exhaust gases against the particle size. Both cars have a unimodal distribution of the surface area around a PMD of 300 nm; the PFI car has a peak value of 1.44×10^4 μm^2/cm^3 and the GDI car a peak value of 3.60×10^5 μm^2/cm^3. Compared with the particle number size distribution shown in Figure 4a, the peak particle surface area for both cars is toward the right (i.e., toward larger particles) and lies in the accumulation mode. Moreover, because far more particles are emitted from the GDI car than from the PFI car, the surface area of GDI particles is evidently higher than that of PFI particles. The metric φ_{SA} has a wide range of 0.57–27.38 for the particle sizes measured. The surfaces of particles originating from automotive vehicles usually absorb and condense many toxic species, such as polycyclic aromatic hydrocarbons, organic compounds and toxic metals. Oberdorster (2001) concluded that the particles with large specific surface area possessed a stronger capacity of adsorbing toxic gaseous materials in atmosphere, resulting in the higher toxicity of particles. Thus, the GDI particles with a larger surface area probably have greater toxic potential than PFI particles.

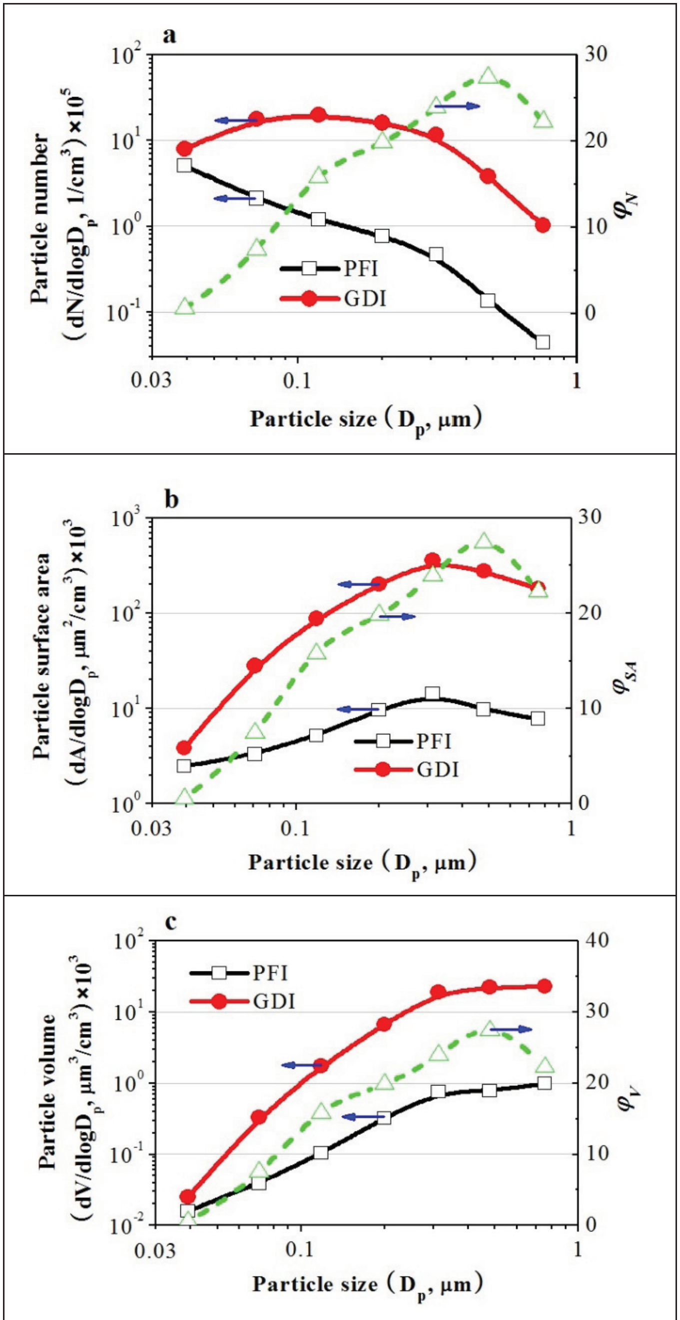

Figure 4. *Comparison of the particle number, surface area and volume distributions under the NEDC.*

In Figure 4c, there is an increase in particle volume with an increase in the particle size for both cars, and the particle volume at the maximum PMD measured (755 nm) is much higher than that at the minimum PMD measured (39 nm). The particle volume is a surrogate for the mass assuming that the particle density does not vary with the size of the emitted particles (Price et al., 2006). The high particle volume density in the range of the large particle sizes suggests that the vast majority of the particle mass is contributed by the larger particles, although most particles by number are in the smaller size range (Figure 4a). Additionally, Figure 4c shows that the particle volume of the GDI car is higher than that of the PFI car over the range of particle sizes measured; φ_V has a wide range of 0.56–27.39. This result indicates that the overall particle mass for the GDI car is much higher than that for the PFI car over the NEDC.

In this paper, the emissions per km were calculated by dividing the sum of particle number, surface area and volume by mileage that the car covered under the NEDC. The emissions per km at particle number, volume and surface area are presented in Table 4. The particle number, volume and surface area for the GDI car are respectively 6.3×10^{12} particles/km, 7.8×10^{-8} m^3/km and 0.392 m^2/km, and respectively 1.0×10^{12} particles/km, 7.8×10^{-9} m^3/km and 0.025 m^2/km for the PFI car. The particle number, volume and surface area per km for the GDI car are respectively 5.3, 9.0 and 14.6 times higher than those for the PFI car. Similar results were reported by Ristimaki et al. (2005). They found that the measured particle number over the ECE15+EUDC cycles were approximately 1.0×10^{13} particles/km for GDI car and 1.4×10^{12} particles/km for PFI car when testing at 266 K. In the study of Maricq et al. (1999b), the particle emission levels of the PFI vehicles were generally in the range of 10^{12}–10^{13} particles/km for the phase 1 of the FTP and US06 drive cycles and 10^{10}–10^{11} particles/km for the phases 2 and 3 of the FTP drive cycle.

Table 4. *Particle emissions for the PFI and GDI cars under the NEDC*

Car Type	PFI	GDI
Particle number (particles/km)	1.0×10^{12}	6.3×10^{12}
Particle volume (m^3/km)	7.8×10^{-9}	7.8×10^{-8}
Particle surface area (m^2/km)	0.025	0.392

3.2. Particle number and size distributions in each segment of the NEDC

We divide the NEDC into its five segments; i.e., ECES1, ECES2, ECES3, ECES4 and EUDC (see Figure 2). The exhaust particle number and size distributions in each segment are shown in Figures 5a and 5b. The patterns of the particle number and size distributions are different for the GDI and PFI cars. In the case of the PFI car (Figure 5a), the particle number distributions under the ECES1 and EUDC decrease with an increase in particle size, and those under the ECES2, ECES3 and ECES4 remain almost at the background concentration levels in the range of particle sizes measured. Moreover, the number concentration of small size particles under the EUDC is higher than that under the ECES1. This can be explained by the occurrence of a high particle spike under the EUDC for the PFI car, and these particle emitted are almost in the small size range. In the case of the GDI car (Figure 5b), all the driving segments are lower for the particle number distributions compared for the ECES1 segment, similar to the common pattern of the diesel particle number distribution (Kittelson, 1998).

In light of the data presented in Figures 5a and 5b, the average particle number concentrations in each driving segment is calculated and illustrated in Figure 5c. Being close to the background concentration, the average particle number concentrations for the PFI car in ECES2–ECES4 are not shown. In each driving segment, the GDI car has an obviously higher average particle number concentration than the PFI car. The average particle number concentration for the GDI car is about 9 times higher than that for the PFI car in ECES1 and 1.7 times higher than that for the PFI car in the EUDC. Moreover, although ECES1–4 run the same ECE–15 segment, ECES1 is found to have the highest particle number concentrations for both the PFI and GDI cars. For the GDI car, the particle number concentration under the cold condition of ECES1 is more than 4 times higher than that under the hot condition of ECES4. The cold start phase (266 K) in the ECES1 segment is responsible for this behavior. Under cold start conditions, on the one hand, fuel vaporization is insufficient and it is necessary for the engine to be run with an over–rich fuel–air mixture for effective combustion (Ohyama et al., 1996; Bielaczyc and Merkisz, 1999), resulting in more particles being emitted. On the other hand, although three–way catalyst (TWC) can oxidize the particles originating from the semi–volatile hydrocarbons, this oxidation reaction hardly takes place when the exhaust temperature is lower than the light–off temperature of TWC, which typically lies between 250 °C and 300 °C (Mathis et al., 2005).

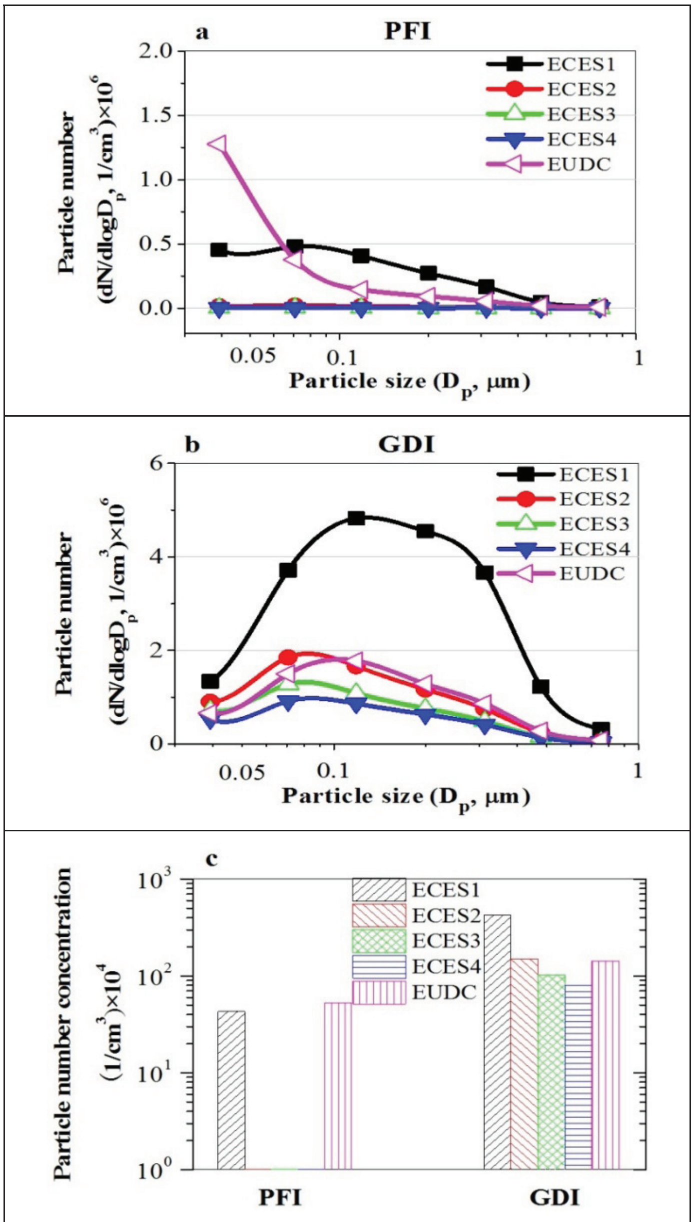

Figure 5. *Characteristics of the exhaust particles in each segment of the NEDC:* ***(a)*** *particle number distribution for the PFI car,* ***(b)*** *particle number distribution for the GDI car,* ***(c)*** *average particle number concentration for both cars.*

3.3. Particle number, surface area and volume under the FSE

As mentioned above, partial or complete misfire, combustion instability and poor effectiveness of after–treatment systems can significantly increase particle emissions from gasoline cars. In this study, such phenomena usually take place in the initial phase of the NEDC (Clairotte et al., 2013). As expected, the highest spike in the time–resolved number concentration shown in Figure 3 was also found in the FSE segment. Therefore, we pay particular attention to the FSE; i.e., the period from 0 to 49 s during the NEDC procedure. More details of the FSE are given in Figure 2, and the particle number distribution and time–resolved particle number under the FSE is shown in Figures 6 and 3. With an increase in particle size, the particle number distribution decreases after an increase for the GDI car, and decreases for the PFI car, similar to what was observed under the other operating conditions in this study. Moreover, the average particle number, surface area and volume concentrations under the FSE and ECES1 are presented in Figures 7a–7c. As expected, both cars emitted a great abundance of particles in the FSE. In the case of the PFI car, the average particle number, surface area and volume concentrations in the FSE were respectively 71.2, 17.3 and 17.6% higher than values in the ECES1. In the case of the GDI car, the corresponding incremental ratios were 65.1, 95.8 and 103.7% respectively. Figures 7a–7c also shows that the data for the GDI car under the FSE are much higher than those for the PFI car under the FSE, by a factor of 9.5 for the average particle number concentration, 33.2 for the surface area concentration and 39.8 for the volume concentration. The explanation for this behavior is consistent with explanations given in Section 3.1, because the combustion mode adopted by the GDI car engine is responsible for the higher particle emissions.

4. Conclusions

The present investigation compared particle emissions from the plumes of PFI and GDI cars. Under all testing conditions, the

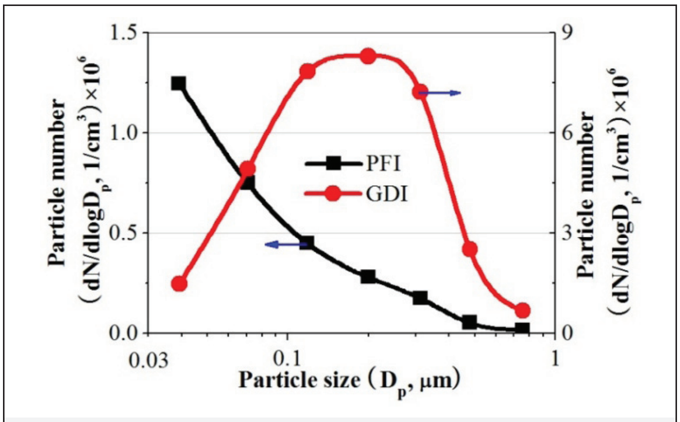

Figure 6. *Comparison of the particle number distributions under the FSE.*

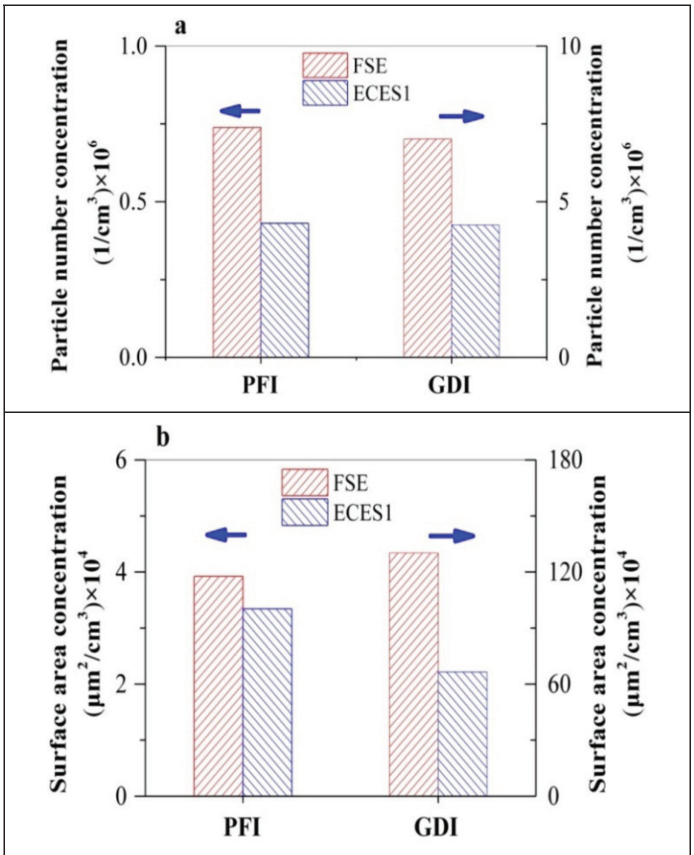

Figure 7. *Comparison of the particle number, surface area and volume concentrations under the FSE and ECES1.*

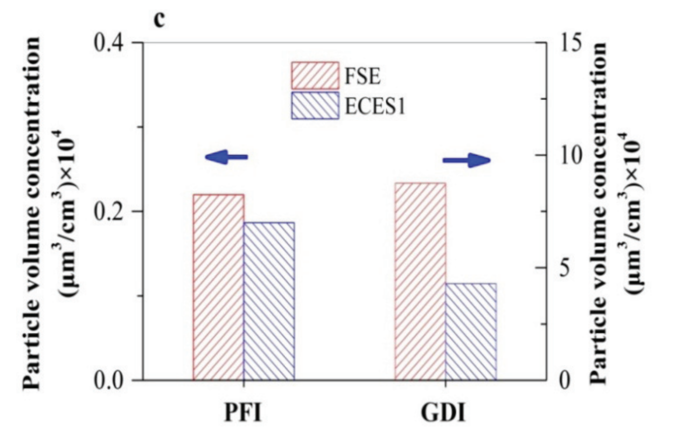

Figure 7. *(Continued).*

GDI car can be characterized by notably higher levels (56–2 739%) of particle emissions in terms of particle number, surface area and volume as compared with the PFI car. Under the NEDC, the particle number, volume and surface area emissions per km for the GDI car are respectively 5.3, 9.0 and 14.6 times those for the PFI car. The particle number distribution of the GDI car initially increases and then decreases with increasing particle size in all the driving segments, similar to a diesel–like pattern of the particle number distribution, while that of the PFI car decreases with an increase in particle size. Among the driving segments employed, the FSE has the highest particle number, surface area and volume concentrations for both the PFI and GDI cars. The size of particles emitted from the PFI car is much smaller than that of particles emitted from the GDI car.

Acknowledgments

This study was supported by the National Key Basic Research and Development Program (2013CB228502), the Tianjin Research Program of Application Foundation and Advanced Technology (10JCZDJC24900) and the Doctoral Program of Higher Education of China (20090032110002).

References

Andersson, J., Wedekind, B., Hall, D., Stradling, R., Wilson, G., 2001. DETR/SMMT/CONCAWE Particulate Research Programme: Light duty results. *SAE International,* art. no. 2001–01–3577.

Bielaczyc, P., Merkisz, J., 1999. Euro III / Euro IV emissions – A study of cold start and warm up phases with a SI (spark ignition) engine. *SAE International,* art. no. 1999–01–1073.

Clairotte, M., Adam, T.W., Zardini, A.A., Manfredi, U., Martini, G., Krasenbrink, A., Vicet, A., Tournie, E., Astorga, C., 2013. Effects of low temperature on the cold start gaseous emissions from light duty vehicles fuelled by ethanol–blended gasoline. *Applied Energy* 102, 44–54.

Eastwood, P., 2008. *Particulate Emissions from Vehicles*, John Wiley & Sons, Inc., New York, pp. 43.

Gupta, T., Kothari, A., Srivastava, D.K., Agarwal, A.K., 2010. Measurement of number and size distribution of particles emitted from a mid–sized transportation multipoint port fuel injection gasoline engine. *Fuel* 89, 2230–2233.

Hoek, G., Brunekreef, B., Goldbohm, S., Fischer, P., van den Brandt, P.A., 2002. Association between mortality and indicators of traffic–related air pollution in the Netherlands: A cohort study. *Lancet* 360, 1203–1209.

Kayes, D., Hochgreb, S., 1999. Mechanisms of particulate matter formation in spark–ignition engines. 1. Effect of engine operating conditions. *Environmental Science & Technology* 33, 3957–3967.

Kittelson, D.B., 1998. Engines and nanoparticles: A review. *Journal of Aerosol Science* 29, 575–588.

Li, N., Hao, M.Q., Phalen, R.F., Hinds, W.C., Nel, A.E., 2003. Particulate air pollutants and asthma – a paradigm for the role of oxidative stress in PM–induced adverse health effects. *Clinical Immunology* 109, 250–265.

Liang, B., Ge, Y.S., Tan, J.W., Han, X.K., Gao, L.P., Hao, L.J., Ye, W.T., Dai, P.P., 2013. Comparison of PM emissions from a gasoline direct injected (GDI) vehicle and a port fuel injected (PFI) vehicle measured by electrical low pressure impactor (ELPI) with two fuels: Gasoline and M15 methanol gasoline. *Journal of Aerosol Science* 57, 22–31.

Mamakos, A., Martini, G., Marotta, A., Manfredi, U., 2013a. Assessment of different technical options in reducing particle emissions from gasoline direct injection vehicles. *Journal of Aerosol Science* 63, 115–125.

Mamakos, A., Steininger, N., Martini, G., Dilara, P., Drossinos, Y., 2013b. Cost effectiveness of particulate filter installation on direct injection gasoline vehicles. *Atmospheric Environment* 77, 16–23.

Maricq, M.M., Podsiadlik, D.H., Brehob, D.D., Haghgooie, M., 1999a. Particulate emissions from a direct–injection spark ignition (DISI) engine. *SAE International,* art. no. 1999–01–1530.

Maricq, M.M., Podsiadlik, D.H., Chase, R.E., 1999b. Gasoline vehicle particle size distributions: Comparison of steady state, FTP, and US06 measurements. *Environmental Science & Technology* 33, 2007–2015.

Mathis, U., Mohr, M., Forss, A.–M., 2005. Comprehensive particle characterization of modern gasoline and diesel passenger cars at low ambient temperatures. *Atmospheric Environment* 39, 107–117.

Ntziachristos, L., Mamakos, A., Samaras, Z., Mathis, U., Mohr, M., Thompson, N., Stradling, R., Forti, L., Serves, C., 2004. Overview of the European "Particulates" project on the characterization of exhaust particulate emissions from road vehicles: Results for light–duty vehicles. *SAE International,* art. no. 2004–01–1985.

Oberdorster, G., 2001. Pulmonary effects of inhaled ultrafine particles. *International Archives of Occupational and Environmental Health* 74, 1–8.

O'Connor, G.T., Neas, L., Vaughn, B., Kattan, M., Mitchell, H., Crain, E.F., Evans, R., Gruchalla, R., Morgan, W., Stout, J., Adams, G.K., Lippmann, M., 2008. Acute respiratory health effects of air pollution on children with asthma in US inner cities. *Journal of Allergy and Clinical Immunology* 121, 1133–1139.

Ohyama, Y., Yamauchi, T., Ohsuga, M., 1996. Mixture formation during cold starting and warm–up in spark ignition engines. *SAE International,* art. no. 960065.

Peters, A., Liu, E., Verrier, R.L., Schwartz, J., Gold, D.R., Mittleman, M., Baliff, J., Oh, J.A., Allen, G., Monahan, K., Dockery, D.W., 2000. Air pollution and incidence of cardiac arrhythmia. *Epidemiology* 11, 11–17.

Price, P., Stone, R., Collier, T., Davies, M., 2006. Particulate matter and hydrocarbon emissions measurements: Comparing first and second generation DISI with PFI in single cylinder optical engines. *SAE International,* art. no. 2006–01–1263.

Ristimaki, J., Keskinen, J., Virtanen, A., Maricq, M., Aakko, P., 2005. Cold temperature PM emissions measurement: Method evaluation and application to light duty vehicles. *Environmental Science & Technology* 39, 9424–9430.

Ronkko, T., Pirjola, L., Ntziachristos, L., Heikkila, J., Karjalainen, P., Hillamo, R., Keskinen, J., 2014. Vehicle engines produce exhaust nanoparticles even when not fueled. *Environmental Science & Technology* 48, 2043–2050.

Samet, J.M., Zeger, S.L., Dominici, F., Curriero, F., Coursac, I., Dockery, D.W., Schwartz, J., Zanobetti, A., 2000. The National Morbidity, Mortality, and Air Pollution Study. Part II: Morbidity and Mortality from Air Pollution in the United States, Research Report of Health Effects Institute, No. 94:5.

Yin, J.X., Harrison, R.M., 2008. Pragmatic mass closure study for $PM_{1.0}$, $PM_{2.5}$ and PM_{10} at roadside, urban background and rural sites. *Atmospheric Environment* 42, 980–988.

Zhao, F., Lai, M.C., Harrington, D.L., 1999. Automotive spark–ignited direct–injection gasoline engines. *Progress in Energy and Combustion Science* 25, 437–562.